An Image Processing Algorithm to Optimize the Output Configuration of a Photonic Integrated Circuit

Luca Gemma[1], Martino Bernard[2], and Davide Brunelli[1]

[1] Department of Industrial Engineering,
University of Trento, I-38123 Povo, Italy
[2] Centre for Sensors and Devices,
Fondazione Bruno Kessler, I-38123 Povo, Italy

Abstract. The interest in silicon photonics as a quantum enabling technology is rapidly growing, and Photonic Integrated Chips (PICs) have been proven to be a robust and viable solution in such research fields. As this technology applied to the quantum world is relatively young, some areas of interest remain uninspected, especially the control and output optimization. In this work, we propose an image processing tool to control and optimize a PIC based solely on images captured by a camera and without invasive output detectors. We tested this architecture on a Silicon Oxynitride (SiON) PIC where several Mach-Zehnder interferometers can be voltage driven by Titanium-Titanium Nitride (TiTiN) thermistors. By comparing the results of the image processing algorithm with those retrieved by silicon photodetectors on the same chip, we have proven that our approach can match or even outperform the traditional approach of sensing outputs with silicon photodetectors.

Keywords: quantum circuits, PIC, image processing, optimization algorithm

1 Introduction

Quantum advantage has been claimed by different quantum technologies: in 2019, Sycamore, Google's quantum computer, solved in 200 seconds a problem that would have taken Summit, the fastest non-quantum computer, at least two days to resolve [16]. In 2020, Jiuzhang, a photonic-based quantum computer, solved the boson sampling problem, which would have taken a classical computer nearly 600 million years to solve [9]. Since then, many companies are inspecting different quantum technologies as enablers for quantum computing: IBM [8] and Rigetti [10] with superconducting circuits, QuiX Quantum [15] and PsiQuantum [7] with photonic circuits, DWave [4] with quantum annealing, IonQ [3] with trapped ions and Microsoft [18] with topological systems. Photonic Integrated Circuits (PICs) represent a viable solution to photonic quantum systems as they are based on well-known structures (used, for example, in telecommunications).

They do not require bulky architectures for hard-cooling (as instead superconducting circuits do) and can be embedded almost effortlessly with electronics as their fabrication process has many similarities with the Very Large Scale Integrated (VLSI) circuits. PICs usually require a chain of tunable channels (as shown for example, in [15]), and nowadays, such tuning is not straightforward but requires devices and a specific algorithm for the calibration. This paper proposes an automatic tool to achieve an optimal configuration without the need for bulk and invasive probes or fixed on-chip detectors and for arbitrary inspecting any region of the PIC and thus considering field intensity in arbitrary regions of the PIC as targets to be optimized. We tested the entire toolchain on PICs that we have fabricated in our facilities and compared the performances of the image processing algorithm with an analogue algorithm based on more classical feedback outputs, such as silicon photodetectors embedded in our PICs. This paper is organized as follows: in Section 2 we illustrate the state-of-the-art briefly for silicon photonics in quantum circuits. Section 3 summarizes our hardware and software architecture, focusing on our image processing tool. In Section 4 we illustrate our measurements and how they were achieved. Finally, in Section 5 conclusions are drawn.

2 Related Works

SiN has been proven to be a viable and robust solution for PIC architectures [13], particularly in the near-infrared, where our work is inserted. In addition, PICs are now considered one of the main architectures when dealing with basic quantum building blocks, such as the Mach-Zehnder Interferometers (MZIs) [2], e.g., an effective redundant alternative to beam splitters that allow for controlling both the amplitude and the phase-shift of the light. We based this work on previous studies we have conducted to characterize our output detectors [6], namely silicon photodiodes, and on our phase-shifters [5], i.e., metallic Ti-TiN thermistors. Concerning the layout, we have chosen to follow a Clements architecture, with which it is possible to achieve a compact structure with low propagation losses and a restricted optical depth [11]. Although being a better solution w.r.t. the simpler counterpart, called "Reck" architecture [12], the optimal calibration of such a structure is still an open issue. Even if image processing has already been used for integrated optics, from fiber alignment [14] to defects inspection [17], up to our knowledge, there are still no works proposing a solution based on image processing to calibrate and tune the PIC outputs based on scattering from the waveguide. This paper presents an optical tool to non-invasively retrieve the optical field intensity in arbitrary points within a configurable PIC, thus assessing its state by exploiting light scattering from its waveguides. This tool can be used to assess the state of a Quantum PIC by temporarily injecting laser light in the circuit to assess, map and set the state of the PIC, and then injecting few-photon states for a proper experiment.

3 Architecture

We fabricated our chips at the Bruno Kessler Foundation's (FBK) Sensor and Devices facility [1] on a 150 mm diameter crystalline wafer with a top epitaxially grown Silicon layer. The silicon photodiodes are realized through ion implantation, and an oxide cladding is realized over the substrate. On top of that, a patterned Silicon Oxynitride (SiON) layer constitutes the photonic layer. The photonic layer is then covered by silicon oxide, acting as protection and optical insulation. Finally, thermistors are realized on top, with a stacked layer of Titanium-Titanium Nitride and Titanium (Ti-TiN-Ti). After fabrication and dicing, the chips have all been connected to custom PCBs with wire bonding, each featuring a total of 10 MZIs with 27 thermistors. Thanks to the thermo-optic effect, by acting on our metallic thermistors, it is possible to change the optical path of the injected laser beam by effectively changing the refractive index of local regions of the waveguides. We controlled the thermistors using voltage, and thus, by Joule's effect, dissipating power and locally generating heat; such control is described in Fig. 1 where from a rest state of equally distributed output intensities, the system moves to a configuration where just a specific branch of an MZI (in (a)) or output of the entire system (in (b)) is active. The optical tool we built is based on images taken from the live stream of a Thorlabs camera which captures the image of a portion of the PIC from above. All the project is based on Python 3.9. We controlled our DoFs (i.e., the phase-shifters) through a Q8b driver model and its custom python module. For validating the approach, a 2450 Keithley digital multimeter was connected to the silicon photodiode of the target output to be optimized, using the PyVisa library to interface and control the instrument. The Opencv cv2 library was used for all the image processing operations. Throughout all our work, we aimed to find the best combination of drive voltages for the thermistors that better maximized the light intensity of a target output. The algorithm is briefly discussed as follows: first of all, a target output combination is specified through a vector with either "1" (in case of maximization) or "0" (for minimization). For our experiments, such a target vector was composed of a single "1" and all other elements set to "0" (i.e., we look for maximizing a single output and minimizing all the other ones). Then an image of the excited PIC is acquired. From the image, the field intensity in specific rectangular regions of identical dimensions is estimated as the sum of all the inner pixel values for each of such regions. An additional "dark" region, far from the waveguides, is acquired and used as a background correction to compensate for possible changes in the light conditions. Therefore, we compute the offset as the sum of the inner pixel values for a "dark" region, and then we subtract it from each region. The measured outputs (i.e., the computed pixel values for each region) are then assembled in a measured output vector. Finally, the measured output vector is normalized to unity to be comparable with the target output vector. A cost function is applied to the target and measured output vectors, which minimizes the norm of the difference between these two vectors. A similar approach is used to realize a twin set of data by using an integrated photodiode to estimate the state of the "1" output channel. To compare the optical tool we

developed with the classical approach of on-chip sensing, we then developed an algorithm to retrieve the current measurements sensed by the digital multimeter connected to the output to be maximized and look for the combination of drive voltages that better maximized such current readings.

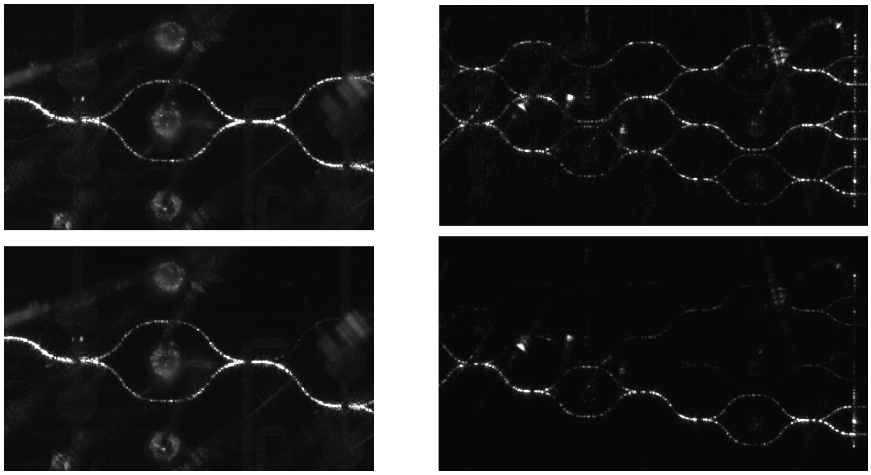

(a) single MZI (b) entire architecture

Fig. 1: Single MZI actuation (a): from an almost 50:50 split ratio (top) to a full transfer (bottom). Full architecture (b): from equally distributed output intensities (top) to a specific target output (bottom).

4 Results

We tested a Silicon Nitride PIC by controlling the 27 metallic thermistors, thus effectively achieving a 27 DoFs system and sensing one output at a time through 2450 Keithley digital multimeter connected to the respective silicon photodiode. The light beam was generated through a near-infrared 850 nm laser. We conducted two types of measurements: in the first set, the image processing tool was used to optimize (thus maximize) a target output, then a second set was produced as a reference and performance comparison by running the same optimization algorithm but based on sensed photocurrents from a single photodiode polarized in reverse bias at -3V [6], thus optimizing the same target output, which in turn means minimizing it (as the measurement is conducted in inverse polarization). In both cases, we controlled our thermistors by providing a 0 to 12V voltage sweep with a step of 0.5V. Each set of measurements was conducted for different input-output combinations, keeping the same configuration between the first and the second set.

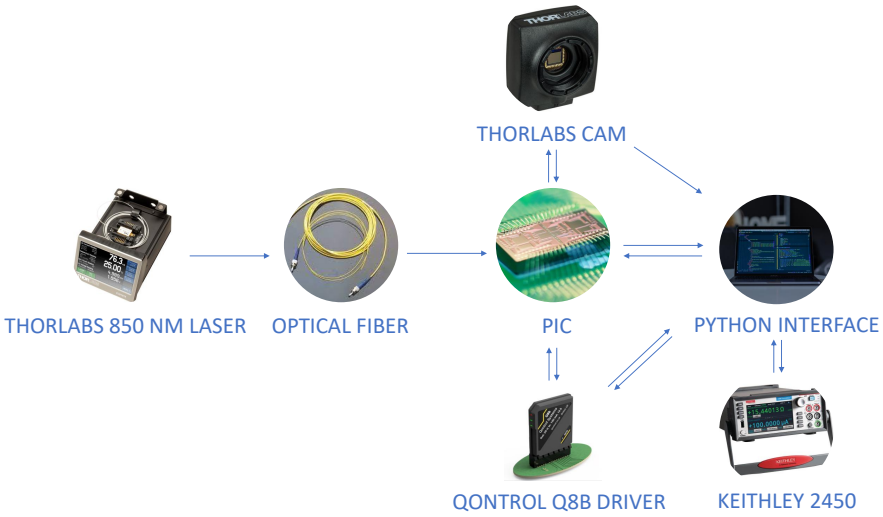

Fig. 2: System architecture.

For the sake of clarity for the reader, it is worth noting that we enumerate our inputs and outputs from bottom to top; thus, input (or output) 1 is the bottom one, and input (or output) 6 is the top one. We report the results obtained for one of the middle inputs (input 4) as this represents a scenario involving one of the highest combinations of degrees of freedom to be controlled and optimized. The starting configuration is shown in Fig.3, where it can be noted that the majority of the incoming NIR beam is routed, due to the uncontrolled initial state of the system, into the last top couple branches (output 5 and 6). The image processing-based optimization algorithm was then run on such configuration specifying as target output configuration a maximization of output 4 and minimization for all the remaining outputs. The estimated pixel intensities evolution during optimization for each outputs are shown in section (a) of Fig.4. On the y-axis, the computed pixel intensity sum is displayed as a function of the evolution coordinate (i.e., image number) as each voltage sweep is performed on all detected DoFs. It is worth noting that after each V-shaped curve (that represents a sweep for a single thermistor), the information about the optimization is preserved: after each maximization (red line), the signal jumps to the local maximum (i.e., the highest value reached during the single sweep) while after each minimization (all other colored lines) the signal jumps to the local minimum (i.e., the lowest value achieved). This means that the system is correctly set to the optimal local configuration reached during each sweep. The final maximization (i.e., the optimization of the output 4, in red) achieved reached more than twice the starting value and, generally, the minimization routines performed well, with two outputs (5 and 6, respectively in purple and brown) dramatically decreased,

and two outputs (1 and 2, blue and orange) almost kept constant. Although the behavior of output 3 (in green) was counter-trend compared with the other minimizations, this trend can be simply explained by considering that such output is correlated to output 4 (i.e., the one to be maximized) as they lie on the same output branch. Further considerations can be made on the presence of negative values: this is an artifact due to the subtraction of a "dark" computed in a single region, which can reasonably have a different background level with respect to the probe regions, and thus it is possible for the background-subtracted value to fall below zero. This issue can be addressed in future implementations with region-wise dark subtraction. The same experiment was then repeated with the Keithley-based optimization algorithm (section (b) in Fig.4), which aimed at maximizing output 4 by sensing the photocurrent in the reverse bias region of a silicon photodiode coupled with the waveguide. As previously stated, although this is a maximization task, the actual task is to maximize the modulus of the negative photocurrent as the experiment is conducted in reverse polarization, and therefore it appears as a minimization task in the image. Similarly to the image processing case, also in this scenario, the maximization trend is visible throughout the entire experiment, with the algorithm keeping the best (lowest) value reached during every single sweep, confirming the correct functioning of the optimization algorithm. Moreover, the result of the maximization procedure is really similar (about twice the starting value) to what we obtained with the optical tool, confirming the effectiveness of the optical tool as a viable and strong alternative to the more invasive and limited classical approach. The similarities of the final configurations can be seen in Fig.3 where the image processing tool outcome (b) is notably similar to the Keithley-based one (c), and both achieve the goal of successfully maximizing output 4, thus again validating our developed optical tool.

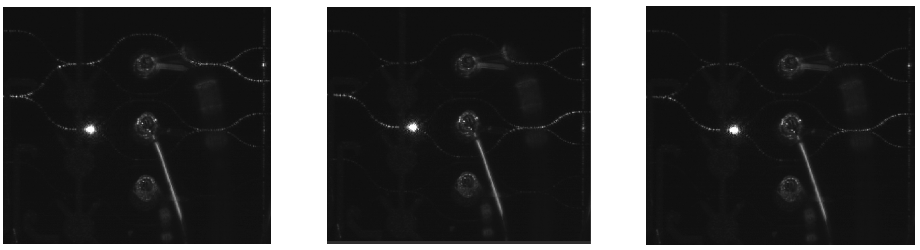

(a) Starting Image

(b) End image Image processing

(c) End image Keithley

Fig. 3: Starting configuration for input 4 and output 4 (a). Final configuration after image processing tool (b) and Keithley-based tool (c).

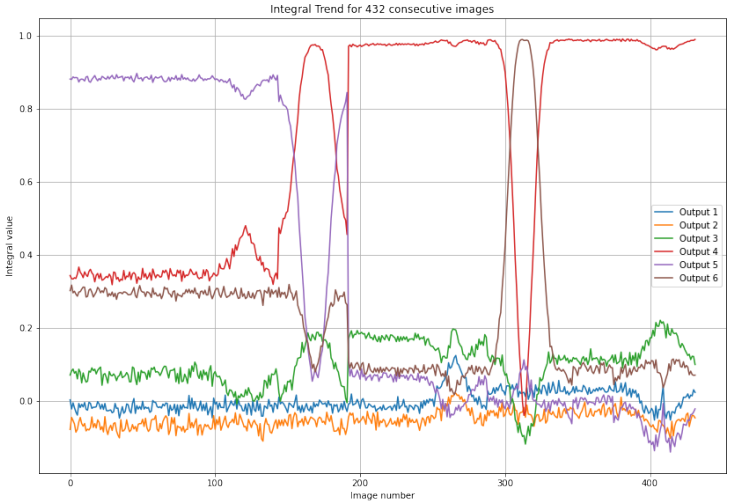

(a) Image Processing

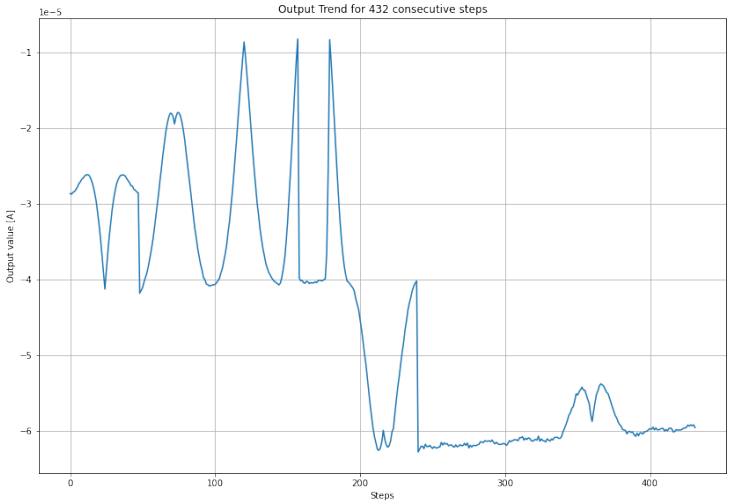

(b) Keithley

Fig. 4: Optimization plots for input 4 and output 4: image processing showing estimated pixel intensities for all outputs (a) and Keithley-based showing sensed photocurrent in reverse bias (b).

5 Conclusions and Future Work

This paper presents an optical tool based on image processing to automatically control and tune multiple outputs of a PIC architecture. This approach has been proven to achieve comparable results w.r.t. a classical sensor-based approach with silicon photodiodes. Moreover, a considerable advantage of this new solution is the ability to inspect and tune intermediate MZI outputs, which are, in general, not easily or arbitrarily accessible with monitor photodiodes. In conclusion, this tool can offer a valid alternative to invasive on-chip detectors. Future work can include the addition of further intelligence to the algorithm in order to automatically identify the best combination of degrees of freedom to use for each specific input/output combination (up to now, this is done by hand by the user as it involves non-trivial considerations of path choices). Moreover, an interesting work would be inspecting the impact of machine learning algorithms on the optimization algorithm itself, e.g., adding a Convolutional Neural Network (CNN) for the image processing tool.

Acknowledgments. We acknowledge the support of the MNF Laboratory staff of FBK during sample fabrication. We acknowledge financial support from the Autonomous Province of Trento, under the initiative *"Quantum at Trento - Q@TN"*, projects *Q-PIXPAD* and *CoSiQuP*. This project has received funding from the European Union's Horizon 2020 research and innovation programme under grant agreements No 777222, ATTRACT *INPEQuT and No 899368,* EPIQUS.

References

1. Sensor and devices, fondazione bruno kessler, https://sd.fbk.eu/en/about-us/
2. Annoni, A., Guglielmi, E., Carminati, M., Grillanda, S., Ciccarella, P., Ferrari, G., Sorel, M., Strain, M.J., Sampietro, M., Melloni, A., Morichetti, F.: Automated routing and control of silicon photonic switch fabrics. IEEE Journal of Selected Topics in Quantum Electronics 22(6), 169–176 (Nov 2016)
3. Blümel, R., Grzesiak, N., Nguyen, N.H., Green, A.M., Li, M., Maksymov, A., Linke, N.M., Nam, Y.: Efficient stabilized two-qubit gates on a trapped-ion quantum computer. Physical Review Letters 126(22) (jun 2021),
4. Boothby, K., Enderud, C., Lanting, T., Molavi, R., Tsai, N., Volkmann, M.H., Altomare, F., Amin, M.H., Babcock, M., Berkley, A.J., Aznar, C.B., Boschnak, M., Christiani, H., Ejtemaee, S., Evert, B., Gullen, M., Hager, M., Harris, R., Hoskinson, E., Hilton, J.P., Jooya, K., Huang, A., Johnson, M.W., King, A.D., Ladizinsky, E., Li, R., MacDonald, A., Fernandez, T.M., Neufeld, R., Norouzpour, M., Oh, T., Ozfidan, I., Paddon, P., Perminov, I., Poulin-Lamarre, G., Prescott, T., Raymond, J., Reis, M., Rich, C., Roy, A., Esfahani, H.S., Sato, Y., Sheldan, B., Smirnov, A., Swenson, L.J., Whittaker, J., Yao, J., Yarovoy, A., Bunyk, P.I.: Architectural considerations in the design of a third-generation superconducting quantum annealing processor (2021), https://arxiv.org/abs/2108.02322

5. Gemma, L., Bernard, M., Ghulinyan, M., Brunelli, D.: Analysis of control and sensing interfaces in a photonic integrated chip solution for quantum computing. In: Proceedings of the 17th ACM International Conference on Computing Frontiers. p. 245–248. CF '20, Association for Computing Machinery, New York, NY, USA (2020), https://doi.org/10.1145/3387902.3394034
6. Gemma, L., Bernard, M., Ghulinyan, M., Brunelli, D.: Analysis of photodiode sensing devices in a photonic integrated chip solution for quantum computing. In: 2020 IEEE SENSORS. pp. 1–4. IEEE (2020)
7. Kim, I.H., Liu, Y.H., Pallister, S., Pol, W., Roberts, S., Lee, E.: Fault-tolerant resource estimate for quantum chemical simulations: Case study on li-ion battery electrolyte molecules. Physical Review Research 4(2), 023019 (2022)
8. Liu, Y., Minev, Z., McConkey, T., Gambetta, J.: Design of interacting superconducting quantum circuits with quasi-lumped models. Bulletin of the American Physical Society (2022)
9. Nature: Light on quantum advantage (2021), https://www.nature.com/articles/s41563-021-00953-0ref-CR3
10. O'Brien, W., Vahidpour, M., Whyland, J.T., Angeles, J., Marshall, J., Scarabelli, D., Crossman, G., Yadav, K., Mohan, Y., Bui, C., Rawat, V., Renzas, R., Vodrahalli, N., Bestwick, A., Rigetti, C.: Superconducting caps for quantum integrated circuits (2017), https://arxiv.org/abs/1708.02219
11. Pérez, D., Gasulla, I., Mahapatra, P.D., Capmany, J.: Principles, fundamentals, and applications of programmable integrated photonics. Adv. Opt. Photon. 12(3), 709–786 (Sep 2020), http://opg.optica.org/aop/abstract.cfm?URI=aop-12-3-709
12. Reck, M., Zeilinger, A., Bernstein, H.J., Bertani, P.: Experimental realization of any discrete unitary operator. Phys. Rev. Lett. 73, 58–61 (Jul 1994), https://link.aps.org/doi/10.1103/PhysRevLett.73.58
13. Roeloffzen, C.G.H., Hoekman, M., Klein, E.J., Wevers, L.S., Timens, R.B., Marchenko, D., Geskus, D., Dekker, R., Alippi, A., Grootjans, R., van Rees, A., Oldenbeuving, R.M., Epping, J.P., Heideman, R.G., Wörhoff, K., Leinse, A., Geuzebroek, D., Schreuder, E., van Dijk, P.W.L., Visscher, I., Taddei, C., Fan, Y., Taballione, C., Liu, Y., Marpaung, D., Zhuang, L., Benelajla, M., Boller, K.: Low-loss si3n4 triplex optical waveguides: Technology and applications overview. IEEE Journal of Selected Topics in Quantum Electronics 24(4), 1–21 (July 2018)
14. Samad, A.A., Unni, C.: Image processing based end-view alignment for symmetric specialty optical fibers. In: 2018 Second International Conference on Inventive Communication and Computational Technologies (ICICCT). pp. 1080–1082 (2018)
15. Taballione, C., Anguita, M.C., de Goede, M., Venderbosch, P., Kassenberg, B., Snijders, H., Kannan, N., Smith, D., Epping, J.P., van der Meer, R., Pinkse, P.W.H., Vlekkert, H.v.d., Renema, J.J.: 20-mode universal quantum photonic processor (2022), https://arxiv.org/abs/2203.01801
16. Times, N.Y.: Why google's quantum supremacy milestone matters (2019), https://www.nytimes.com/2019/10/30/opinion/google-quantum-computer-sycamore.html
17. Vahabi, N., Yang, D., Selviah, D.R.: Improving data transmission in fiber optics by detecting scratches on the fiber end face. In: 2018 IEEE British and Irish Conference on Optics and Photonics (BICOP). pp. 1–4 (2018)
18. Vaitiekėnas, S., Winkler, G.W., van Heck, B., Karzig, T., Deng, M.T., Flensberg, K., Glazman, L.I., Nayak, C., Krogstrup, P., Lutchyn, R.M., Marcus, C.M.: Flux-induced topological superconductivity in full-shell nanowires. Science 367(6485), eaav3392 (2020), https://www.science.org/doi/abs/10.1126/science.aav3392